

## **MALDI-MSI: Biomarker Discovery for Radiation Exposures**

Claire L. Carter<sup>1</sup>, Thomas J. MacVittie<sup>2</sup>, Maureen A. Kane<sup>1</sup>

1. Department of Pharmaceutical Sciences, University of Maryland School of Pharmacy, Baltimore, MD 21201
2. Department of Radiation Oncology, University of Maryland, School of Medicine, Baltimore, MD 21201

### **Radiation Exposures**

Once outside of the Earth's atmosphere astronauts are exposed to two main types of radiation, galactic cosmic rays (GCR) and solar energetic particles. GCRs consist of high energy, charged nuclei of elements ranging from H (hydrogen) to Fe (iron). High energy, charged nuclei of H (protons) are the major component of GCRs whereas approximately 1% of GCRs are larger ions with charges greater than 2+, which are referred to as ions of high (H) atomic number (Z) and energy (E) or HZE ions. Solar energetic particles which occur during solar particle events (SPE) are dominantly protons<sup>[1]</sup>. Due to the differences in radiation type, dose-rate and energy that astronauts experience compared to radiation encountered on Earth, relatively little is known about the biological effects of exposure during manned space missions. Additionally, much of the current models used to calculate exposure risk are based on extrapolated data obtained on Earth<sup>[2]</sup>. Increased risk of cancer, CNS disease and cataracts are real-life issues faced by astronauts. Radioactive material has also been used for decades in industry, medicine and weapons of mass destruction. Radiation exposure (accidental or deliberate) as well as radiation therapy used to treat lung cancers often results in radiation-induced lung injury (pneumonitis and fibrosis), which can be fatal<sup>[3]</sup>. The need for medical countermeasures (MCM) for treatment or mitigation in the event of accidental or intentional radiation exposures is evident. In order to develop MCMs, a clearer understanding of the mechanisms of action by which radiation induces tissue/organ damage is needed, as currently these mechanisms remain incompletely understood. What is evident through the literature in both space radiation and terrestrial radiation studies is that oxidative stress/damage plays a central role in pathologies, and many of the countermeasures evaluated to date have been antioxidants<sup>[1,4]</sup>. The identification of biomarkers for radiation damage/syndromes will not only enable the development and evaluation of MCMs, but also aid in identifying biological readouts that will allow for efficient diagnosis following exposures, which may be vital for survival.

One technique that can greatly contribute to deciphering and understanding the mechanism of action of radiation damage following exposure is matrix-assisted laser desorption/ionization mass spectrometry imaging (MALDI-MSI). Mass spectrometry imaging is a unique technique due to its ability to simultaneously detect and localize hundreds of molecules from an organ section or biopsy, in a single experiment, and without the need of a label or a predefined target. No other technique, as of yet, offers this ability.

### **MALDI-MSI – Applications**

MALDI-MSI is an established technique that is being applied to clinical/disease state samples to investigate mechanism of action and identify biomarkers. It is also being used for drug distribution and efficacy studies, following drug development and treatment regimes. For more

in-depth information of the many fields MSI is now being applied to, the more interested reader is directed to the following review articles<sup>[5-9]</sup>. **Table 1** lists some of the diverse areas to which MSI has been applied.

Tissue Type	Disease	Molecules Identified/Studied	Reference
Esophagus	Barrett's Adenocarcinoma	Proteins	[10]
Colon	Colon Cancer	Proteins	[11]
Brain	Cortical Spreading Depression	Proteins, peptides, metabolites	[12]
Cartilage	Osteoarthritis	Proteins, peptides, metabolites	[13]
Mammary	Breast Cancer	Proteins, peptides, lipids	[14-15]
Colorectal	Cancer	Lipids	[16]
Kidney	Polycystic Kidney Disease	Lipids	[17]
Heart	Myocardial Infarction	Lipids	[18]
Lung	Tuberculosis	Drug distribution, lipids	[19]
Lung	Pulmonary Infection	Proteins	[20]
Lung	Lung Cancer	Drug distribution	[21]
Lung	Lung Cancer	Proteins	[22-23]

**Table 1.** Summary of the different types of tissues/areas of research to which MSI has been applied.

## Overview of MALDI-MSI

Matrix-assisted laser desorption/ionization (MALDI) mass spectrometry imaging (MSI) is an established technique that enables the detection and localization of proteins, peptides, lipids, metabolites, and drugs within organ sections for (patho)physiological processes<sup>[5]</sup>. MALDI is a soft ionization technique introduced first by Karas and Hillenkamp<sup>[24]</sup>, and then Tanaka<sup>[25]</sup>, in the late 1980's. An in-depth description of the MALDI technique is out of the scope of this review, but the interested reader is directed to Tanaka's 2002 Nobel Prize acceptance speech for the application of MALDI to high molecular weight molecules<sup>[26]</sup>, and the dedicated work of Karas and Hillenkamp<sup>[27]</sup>. Briefly, MALDI involves the use of a matrix compound, usually a low molecular weight organic acid, which is mixed in molar excess with the analyte/s (molecule/s) of interest; this is then spotted onto a stainless steel target plate and allowed to air dry, resulting in the formation of a co-crystallized structure of matrix/analyte. The target plate is then placed into the MALDI ion source, and interrogated with a pulsed UV or IR laser. The matrix is required to facilitate desorption/ionization of the molecular species of interest by absorbing the laser energy thereby protecting the molecules from thermal/metastable decay, hence the term soft ionization. The matrix acts as a proton donor/acceptor, thus promoting ionization. Energy transfer from the laser into the co-crystallized structure results in desorption of both the matrix and analyte species from the surface, and the formation of the 'MALDI plume', which contains gas phase (de)protonated and cationized species. Charged species are extracted into the mass analyzer using a known electrical field, where they are separated and detected according to their mass-charge ratio ( $m/z$ )<sup>[27]</sup>.

The MALDI-MSI technique was pioneered by Caprioli and co-workers in 1997, in which they demonstrated imaging of proteins in tissue<sup>[28]</sup>. The same principles behind MALDI apply to MALDI-MSI; a matrix is required to co-crystallize with the analyte/s of interest. For imaging investigations, organs/tissues of interest are sectioned using a cryostat, usually at a thickness between 5 and 20 $\mu\text{m}$ . The sectioned tissue is then transferred onto a MALDI stainless steel sample plate or an indium tin oxide (ITO) coated glass slide, and allowed to dry onto the plate prior to matrix application. Matrix deposition for imaging experiments is more commonly carried out using an artistic airbrush, TLC sprayer, or more recently automated deposition devices and sublimation. The matrix solution is deposited over the target plate and tissue area in the form of a fine mist, with an aim to cover the entire tissue section with a homogenous coating. Matrix deposition has to be carefully optimized, too dry a deposition will lead to inefficient extraction and co-crystallization with the analytes (resulting in poor quality data), whilst a deposition that is too wet will result in delocalization of the analytes across the tissue area (resulting in inaccurate data). Once in the MALDI ion source, a pre-determined data acquisition grid pattern controls the movement of the sample plate within defined x and y dimensions. The sample plate moves under a fixed UV or IR laser and a full mass spectrum of compounds is acquired at each location. The acquired data files are then converted or transferred to an image processing application program. Each laser spot or individual spectrum now becomes a pixel. Imaging applications allow the selection of the  $m/z$  of interest and enables visualization of its distribution over the tissue section. Pixel intensity (given in RGB color scale in many cases) of the analyte/s of interest corresponds to relative ion intensity. Alternately, a pixel or region of interest can be selected and a full mass spectrum from that area can be observed, these can then be compared to other areas/regions, e.g. tumor vs. tumor margin vs. normal tissue. The image resolution selected is dependent upon the diameter of the laser spot and the size of the matrix/analyte co-crystals. Acquisition parameters are generally set between 50-200  $\mu\text{m}$ , with a smaller distance giving higher resolution. More recently, investigators have reported image acquisitions down to 3  $\mu\text{m}$ <sup>[5]</sup>. The workflow from sample preparation to image and spectral analysis is shown in **Figure 1**. Spatial resolution is limited to an extent by the laser diameter and crystal size of the matrix used as previously discussed. Matrix crystal size depends heavily on the method of deposition/sample preparation. Recent advancements in laser technology, instrumentation and automated matrix deposition devices, have greatly improved these spatial limitations and continue to expand the technical capabilities of MSI for determining spatial changes in the anatomical distribution of molecules during pathological conditions, whose amount or quantity may otherwise appear normal in a bulk measurement of total abundance.

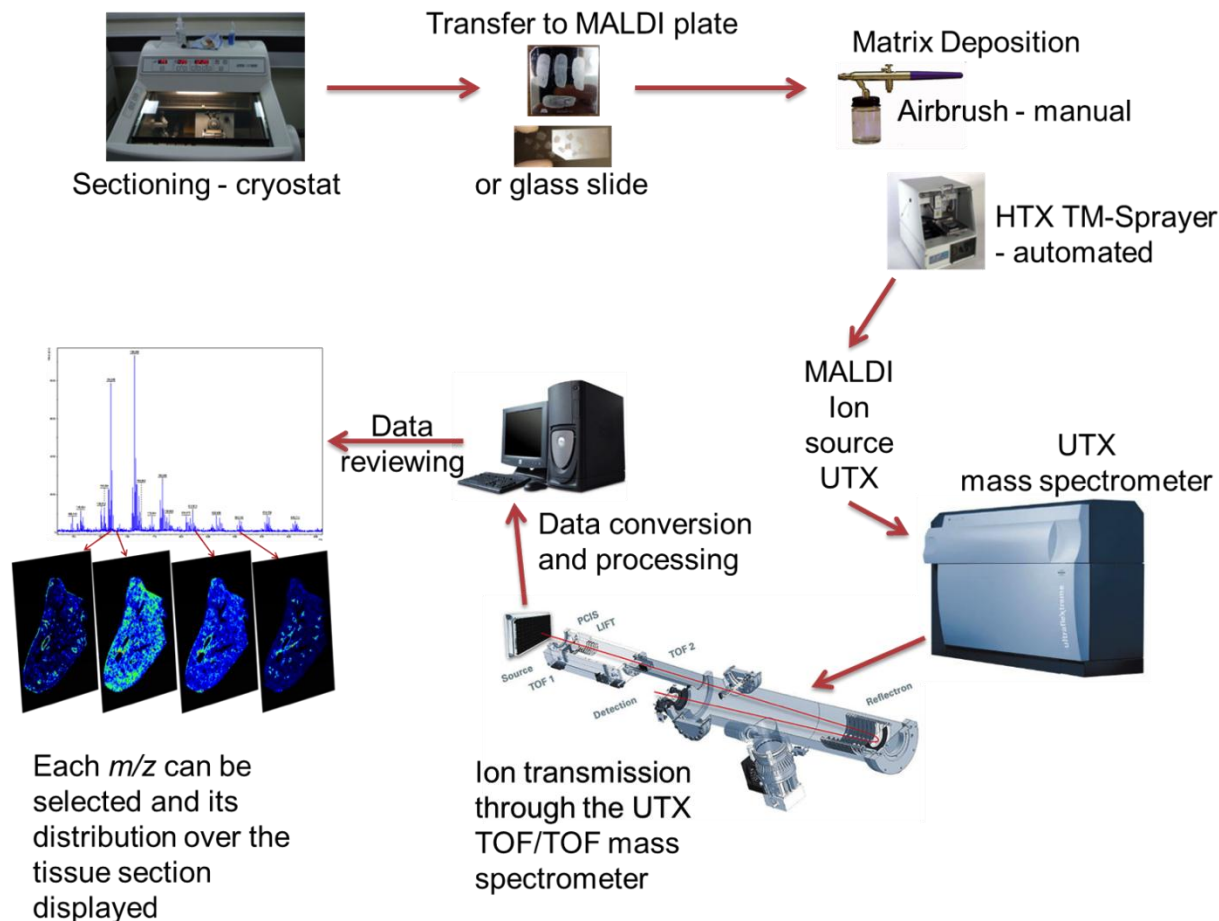


**Figure 1.** MALDI-MSI workflow from sample preparation to analysis.

## MALDI-MSI Application to Radiation Exposure

We are currently applying MALDI-MSI to animal models of acute radiation syndrome (ARS) and the delayed effects of acute radiation exposure (DEARE) to map molecular changes within organ sections following radiation insult, thereby aiding in biomarker identification and definition of potential mechanisms of action for radiation and the MCM. Example MALDI-MSI data showing changes in lipid intensity from a normal lung biopsy and a damaged lung biopsy after a whole thorax lung irradiation (WTLI) dose of 11 Gy is shown in **Figure 2**. The lipid at  $m/z$  734 is a phosphatidylcholine (PC 32:0) and is the primary lipid in lung surfactant; a lipoprotein substance which maintains lung structure and protects against oxidants and bacterial insult, dysfunctional lung surfactant is observed in numerous pulmonary disorders<sup>[29]</sup>. The lipid at  $m/z$  741 (SM 16:0) is the most abundant sphingomyelin in mammalian tissues and the major component of ordered lipid microdomains of the plasma membrane, called lipid rafts, which mediate cell signaling and membrane trafficking<sup>[30,31]</sup>. Reduced plasma membrane SM has been associated with increased inflammation, altered cholesterol homeostasis, and dysregulated apoptotic signaling<sup>[30,31]</sup>. These lipids show a marked decrease in the damaged lung biopsy, demonstrating the usefulness of MALDI-MSI for investigating the distribution of biomolecules in organ sections or biopsy samples following radiation exposure.

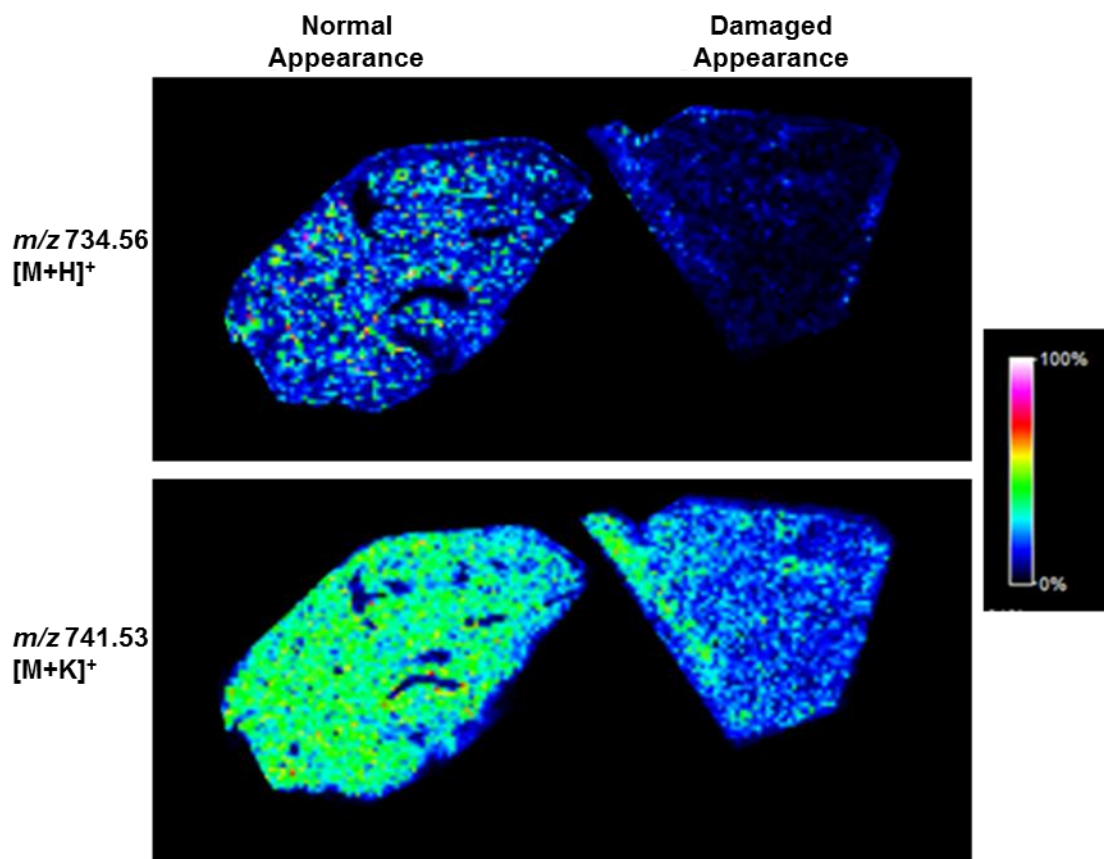


**Figure 2.** MALDI-MSI images of a phosphatidylcholine ( $m/z$  734) and a sphingomyelin ( $m/z$  741) lipid displaying reduced intensity in a lung biopsy that showed histologically abnormal architecture and macrophage infiltration (histology not shown) following radiation. Normal appearing lung biopsies and damaged appearing lung biopsies were collected from the same NHP, after a whole thorax lung irradiation (WTLI) dose of 11 Gy, at day 91 post IR.

Lipids are the main constituent of cellular membranes and are metabolized into important signaling and regulatory molecules, as demonstrated by the schematic in **Figure 3**.

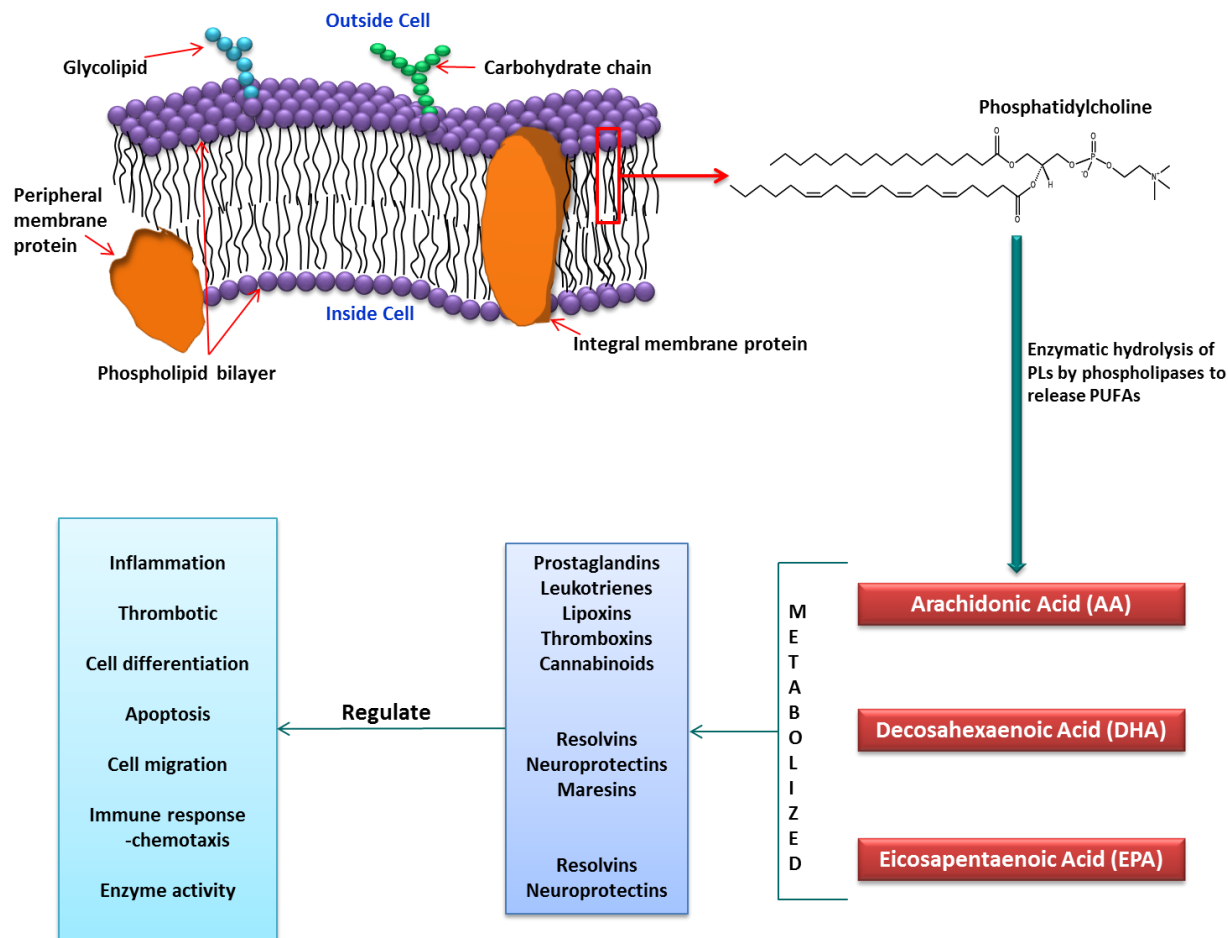


**Figure 3.** Schematic representation of the fluid mosaic model for cell membranes and the importance of lipids during (patho)physiological processes.

### Acknowledgment

This work was funded by the National Institute of Allergy and Infectious Diseases (Contract number HHSN272201000046C). This work was also supported by the University of Maryland School of Pharmacy Mass Spectrometry Center (SOP1841-IQB2014)

### The Future

While MALDI-MSI is not being directly applied to investigating the effects of space radiation yet, the application of MALDI-MSI to radiation models and numerous diseases, including cancer and CNS diseases, will invariably shed light onto the mechanisms of damage caused by space radiation. This will not only help in diagnostics, prognostics and treatment regimens for potential problems that may arise following manned space mission, but may also aid in identifying mitigators that may act to minimize damage following radiation exposures.

## References

- [1] Kennedy, A. R.,; Wan, X. S. Countermeasures for space radiation induced adverse biologic effects. *Advances in Space Research*, 2011. **48**(9): 1460-1479.
- [2] Ding, L. H.,; Park, S.,; Peyton, M.,; Girard, L.,; Xie, Y.,; Minna, J. D.,; Story, M. D. Distinct transcriptome profiles identified in normal human bronchial epithelial cells after exposure to gamma-rays and different elemental particles of high Z and energy. *BMC Genomics*, 2013. **14**(372).
- [3] Hillman, G. G.,; Singh-Gupta, V.,; Lonardo, F.,; Hoogstra, D. J.,; Abernathy, L. M.,; Yunker, C. K.,; Rothstein, S. E.,; Rakowski, J.,; Sarkar, F. H.,; Gadgeel, S.,; Konski, A. A.,; Joiner, M. C. Radioprotection of Lung Tissue by Soy Isoflavones. *Journal of Thoracic Oncology*, 2013. **8**(11): 1356–1364.
- [4] Jackson, I. L.,; Zhang, X. W.,; Hadley, C.,; Rabbani, Z. N.,; Zhang, Y.,; Marks, S.,; Vujaskovic, Z. Temporal expression of hypoxia-regulated genes is associated with early changes in redox status in irradiated lung. *Free Radical Biology and Medicine*, 2012. **53**(2): 337-346.
- [5] Römpf, A.,; Spengler, B. Mass spectrometry imaging with high resolution in mass and space. *Histochemistry and Cell Biology*, 2013. **139**(6): 759-783.
- [6] McDonnell, L. A.,; Heeren, R. M. Imaging mass spectrometry. *Mass spectrometry reviews*, 2007. **26**(4): 606–43.
- [7] Prideaux, B.,; Stoeckli, M. Mass spectrometry imaging for drug distribution studies. *Journal of Proteomics*, 2012. **75**: 4999-5013.
- [8] Neubert, P.,; Walch, A. Current frontiers in clinical research application of MALDI imaging mass spectrometry. *Expert Review of Proteomics*, 2013. **10**(3): 259-273.
- [9] Norris JL, Caprioli RM. Imaging mass spectrometry: a new tool for pathology in a molecular age. *Proteomics Clin Appl*, 2013. **7**(11-12): 733-8.
- [10] Elsner, M.,; Rauser, S.,; Maier, S.,; Schone, C.,; Balluff, B.,; Meding, S.,; Jung, G.,; Nipp, M.,; Sarioglu, H.,; Maccarrone, G.,; Aichler, M.,; Ruchtinger, A.,; Langer, R.,; Jutting, U.,; Feith, M.,; Kuster, B.,; Ueffing, M.,; Zitzelsberger, H.,; Hofler, H.,; Walch, A. MALDI imaging mass spectrometry reveals COX7A2, TAGLN2 and S100-A10 as novel prognostic markers in Barrett's adenocarcinoma. *Journal of Proteomics*, 2012. **75**(15): 4693-4704.
- [11] Meding, S.,; Balluff, B.,; Elsner, M.,; Schone, C.,; Rauser, S.,; Nitsche, U.,; Maak, M.,; Schafer, A.,; Hauck, SM.,; Ueffing, M.,; Langer, R.,; Hofler, H.,; Friess, H.,; Rosenberg, R.,; Walch, A. Tissue-based proteomics reveals FXYD3, S100A11 and GSTM3 as novel markers for regional lymph node metastasis in colon cancer. *Journal of Pathology*, 2012. **288**(4): 459-470.
- [12] Jones, E. A.,; Shyti, R.,; van Zeijl, R. J. M.,; van Heiningen, S. H.,; Ferrari, M. D.,; Deelder, A. M.,; Tolner, E. A.,; van den Maagdenberg, A. M. J. M.,; McDonnell, L. A. Imaging mass spectrometry to visualize biomolecule distributions in mouse brain tissue following hemispheric cortical spreading depression. *Journal of Proteomics*, 2012. **75**(16): 5027-5035.
- [13] Peffers, M. J.,; Cillero-Pastor, B.,; Eijkel, G.,; Clegg, PD.,; Heeren, RM. Ageing and osteoarthritis markers identified by MALDI imaging mass spectrometry. *Osteoarthritis and Cartilage*, 2013. **26**: S63-63.
- [14] Chughtai, K.,; Jiang, L.,; Post, H.,; Winnard, P. T.,; Greenwood, T.R.,; Raman, V.,; Bhujwalla, Z.M.,; Heeren, R. M. A.,; Glunde, K. Mass Spectrometric Imaging of Red

- Fluorescent Protein in Breast Tumor Xenografts. *Journal of the American Society for Mass Spectrometry*, 2013. **24**(15): 711-717.
- [15] Chughtai, K.; Jiang, L.; Greenwood, T. R.; Glunde, K.; Heeren, R. M. A. Mass spectrometry images acylcarnitines, phosphatidylcholines, and sphingomyelin in MDA-MB-231 breast tumor models. *Journal of Lipid Research*, 2013. **54**(2): 333-344.
- [16] Kurabe, N.; Hayasaka, T.; Ogawa, M.; Masaki, N.; Ide, Y.; Waki, M.; Nakamura, T.; Kurachi, K.; Kahyo, T.; Shinmura, K.; Midorikawa, Y.; Sugiyama, Y.; Setou, M.; Sugimura, H. Accumulated phosphatidylcholine (16:0/16:1) in human colorectal cancer; possible involvement of LPCAT4. *Cancer Science*, 2013. **104**(10): 1295-1302.
- [17] Ruh, H.; Salonikios, T.; Fuchser, J.; Schwartz, M.; Sticht, C.; Hochheim, C.; Wirtzner, B.; Gretz, N.; Hopf, C. MALDI imaging MS reveals candidate lipid markers of polycystic kidney disease. *Journal of Lipid Research*, 2013. **54**(10): 2785-94.
- [18] Menger, R. F.; Stutts, W. L.; Anbukumar, D. S.; Bowden, J.A.; Ford, D.A.; Yost, R. A. MALDI Mass Spectrometric Imaging of Cardiac Tissue Following Myocardial Infarction in a Rat Coronary Artery Ligation Model. *Analytical Chemistry*, 2012. **84**(2): 1117-1125.
- [19] Prideaux, B.; Dartois, V.; Staab, D.; Weiner, DM.; Goh, A.; Via, LE.; Barry, C. E.; Stoeckli, M. High-Sensitivity MALDI-MRM-MS Imaging of Moxifloxacin Distribution in Tuberculosis-Infected Rabbit Lungs and Granulomatous Lesions. *Analytical Chemistry*, 2011. **83**(6): 2112-2118.
- [20] Moore JL, Becker KW, Nicklay JJ, Boyd KL, Skaar EP, Caprioli RM. Imaging mass spectrometry for assessing temporal proteomics: Analysis of calprotectin in *Acinetobacter baumannii* pulmonary infection. *Proteomics*. 2013 Jun 11. Epub ahead of print.
- [21] Fehniger, T. E.; Vegvari, A.; Rezeli, M.; Prikk, K.; Ross, P.; Dahlback, M.; Edula, G.; Sepper, R.; Marko-Varga, G. Direct Demonstration of Tissue Uptake of an Inhaled Drug: Proof-of-Principle Study Using Matrix-Assisted Laser Desorption Ionization Mass Spectrometry Imaging. *Analytical Chemistry*, 2011. **83**(21): 8329-8336.
- [22] Rahman SM, Gonzalez AL, Li M, Seeley EH, Zimmerman LJ, Zhang XJ, Manier ML, Olson SJ, Shah RN, Miller AN, Putnam JB, Miller YE, Franklin WA, Blot WJ, Carbone DP, Shyr Y, Caprioli RM, Massion PP. Lung cancer diagnosis from proteomic analysis of preinvasive lesions. *Cancer Res*, 2011. **71**(8): 3009-17.
- [23] Xu BJ, Gonzalez AL, Kikuchi T, Yanagisawa K, Massion PP, Wu H, Mason SE, Olson SJ, Shyr Y, Carbone DP, Caprioli RM. MALDI-MS derived prognostic protein markers for resected non-small cell lung cancer. *Proteomics Clin Appl*, 2008. **2**(10-11): 1508-17.
- [24] Karas, M.; Bachmann, D.; Hillenkamp, F. Influence of the Wavelength in High-Irradiance Ultraviolet Laser Desorption Mass Spectrometry of Organic Molecules. *Analytical Chemistry*, 1985. **57**(14): 2935-9.
- [25] Tanaka, K.; Waki, H.; Ido, Y.; Akita, S.; Yoshida, Y.; Yoshida, T.; Matsuo, T. Protein and Polymer Analyses up to m/z 100 000 by Laser Ionization Time-of flight Mass Spectrometry. *Rapid Communications in Mass Spectrometry*, 1988. **2**(20): 151-3.
- [26] [http://www.nobelprize.org/nobel\\_prizes/chemistry/laureates/2002/tanaka-lecture.html](http://www.nobelprize.org/nobel_prizes/chemistry/laureates/2002/tanaka-lecture.html)
- [27] Hillenkamp, F.; Karas, M.; Beavis, R. C.; Chait, B. T. Matrix-assisted laser desorption/ionization mass spectrometry of biopolymers. *Analytical Chemistry*, 1991 **63**(24): 1193A-1203A.
- [28] Caprioli, R. M.; Farmer, T. B.; Gile, J. Molecular Imaging of Biological Samples: Localization of Peptides and Proteins Using MALDI-TOF MS. *Analytical Chemistry*, 1997. **69** (23): 4751-4760.
- [29] Akella, A.; Deshpande, S. B. Pulmonary surfactants and their role in pathophysiology of lung disorders. *Indian journal of Experimental Biology*, 2013. **51**(1): 5-22.
- [30] Slotte JP. Biological functions of sphingomyelins. *Progress in Lipid Research*. 2013. **52**: 424-437.

- [31] Chakraborty M, Jiang X-C. Sphingomyelin and its role in cellular signaling. Lipid-mediated Protein Signaling. *Advances in Experimental Medicine and Biology*. 2013. **991**: 1-14.